SAND2015-4248C

Macro- and Microscale Particle Size Effects of Soil on Photovoltaic Surfaces

Patrick D. Burton, Alex Hendrickson and Bruce H. King
Sandia National Laboratories
Albuquerque, NM 87185 USA
Email: pdburto@sandia.gov

***Abstract*—The texture or patterning of soil on PV surfaces may influence light capture at various angles of incidence. Accumulated soil can be considered a micro-shading element, which changes with respect to AOI. While scattering losses at this scale would be significant only to the most sensitive devices, micro-shading could lead to hot spot formation and other reliability issues. Indoor soil deposition was used to prepare test coupons for simultaneous AOI and soiling loss experiments. A mixed solvent deposition technique was used to consistently deposit patterned test soils onto glass slides. Transmission decreased as soil loading and AOI increased. Highly dispersed particles are less prone to secondary scattering, improving overall light collection.**

I. Introduction

The accumulation of soil on photovoltaic modules causes a loss in short circuit current due to the reduction in incident light. In order to offset the loss, any mitigation strategy must be resource-effective. Regular washing can be expensive in arid regions [1], so many systems are allowed to soil until naturally cleaned by rain [2]. Unfortunately, light rain or dew can often compound the problem by redispersing and concentrating dust [3]. In addition to the loss in short circuit current, non-uniform soil coverage or irregular shading can cause hot spots [4]–[6] and reduction in voltage [4]. As the angle of incidence changes throughout the day, a non-uniform soil coating will present a different optical profile to the underlying device. Soil particles at the module surface can be thought of as obstacles shadowing the cell. Densely stacked particles could have a greater impact on the underlying cell at high AOI than under direct irradiance.

In order to quantify losses due to irregular soil accumulation, a systematic indoor study was conducted. By controlling particle deposition on glass surfaces, uniform or dispersed soil films were used to simulate a range of soil patterns.

II. Experimental Methods

A. Test Coupon Preparation by Aerosol Spray

Glass slides (Petrographic microscope slides, Ward's Science) were rinsed in DI H_2O, followed by ethanol (EtOH, 200 proof, Sigma Aldrich). Each slide was weighed with a 0.00001 g resolution balance (Mettler Toledo XP205) and placed at a 45° angle inside a filtered spray chamber. A commercial test dust (AZ road dust, Powder Technology Incorporated, ISO 12103-1 A2 Fine) was suspended in a carrier solvent and sprayed on the slide. Ratios of EtOH and acetonitrile (ACN, Reagent Grade, Sigma Aldrich) [0, 20, 40, 60, 80 and 100 % EtOH:ACN] were used as carrier solvents.

B. Test Coupon Preparation by Single Droplet

A variation of this technique was developed to deposit dense soil coatings on small regions of the test coupon. Soil suspensions of 0.01 or 0.02 g/ml were applied using a 10 µl pipette held directly above the slide with a clamp. The soil applied in this manner was below the detectable limit of the mass balance. Samples were quantified by measurement of the dried droplet area only.

For each technique, the area coverage of the applied sand was determined at macroscopic and microscopic length scales using a Canon 10D digital camera and Olympus IX71 microscope equipped with a DP72 camera, respectively. Each image was imported into ImageJ [7] for automated particle analysis. Most single droplets were sufficiently contiguous to measure the entire region using a pixel counting program. For samples with irregular areas, the region of interest (ROI) was outlined by hand and measured.

C. Angle of Incidence

UV/vis/NIR spectroscopic measurements were collected with a Varian Cary 5000 UV/vis/NIR spectrophotometer. Angle of incidence (AOI) effects were evaluated by placing the test slide in a variable angle sample holder in a DRA-2500 diffuse reflectance accessory. Spectra were collected at 10° intervals. Baseline measurements were collected with a clean reference sample mounted in the holder at 0°. This differs from the procedure described by [8] in order to reference all measurements to a perpendicular incident beam. The reference condition thus mimics AM 0 geometry. Transmittance was calculated for spot-soiled samples by collecting one scan with the integrating sphere closed, capturing both transmittance and reflectance data simultaneously, as described in eq. (1). The sample reflectance port was subsequently replaced with a light trap, ensuring that only the scattered light was collected (eq. (2)). Transmittance was calculated using the coupled equations shown in eq. (3).

$$A_1 = -\log(T + R) \quad (1)$$

$$A_2 = -\log(R) \quad (2)$$

$$T = \exp(-A_1) - \exp(-A_2) \quad (3)$$

III. Results and Discussion

Commercial petrography slides were used for compatibility with the variable angle clip holder spectroscopy accessory.

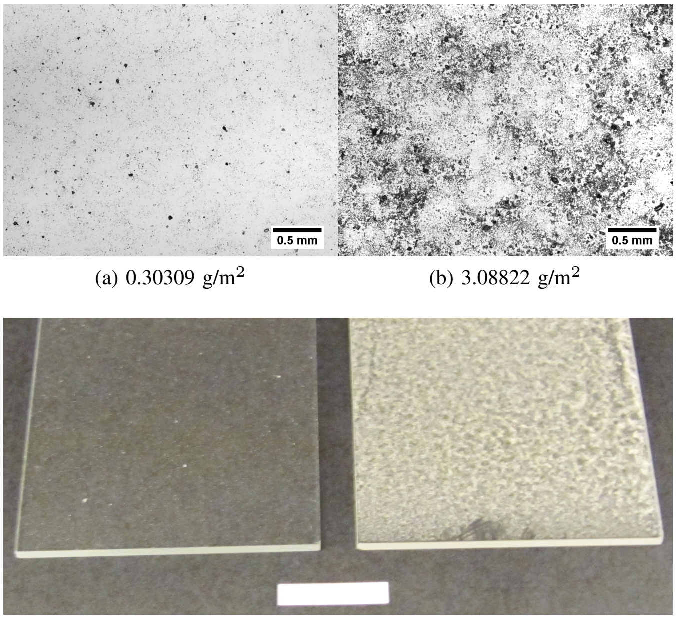

(a) 0.30309 g/m^2 (b) 3.08822 g/m^2

(c) Scale bar = 1 cm

Fig. 1. Light and heavily soiled coupons coated using 100% EtOH carrier solvent.

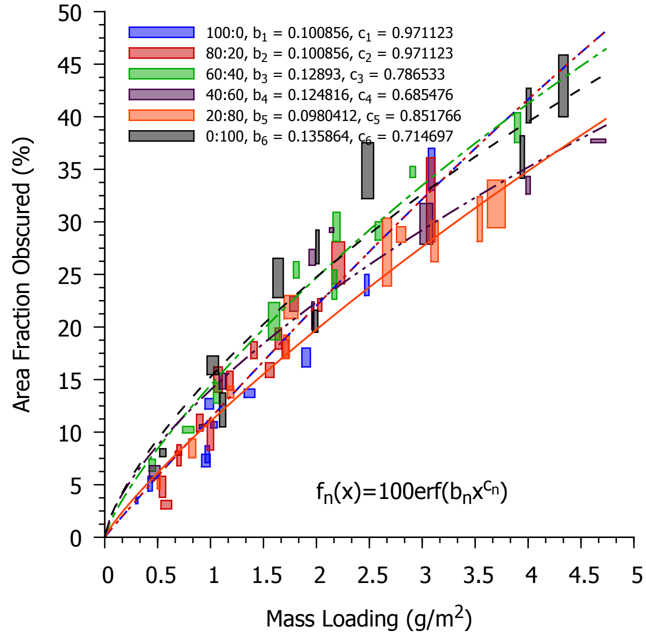

Fig. 2. Correlation between mass loading and obscured area fraction.

These slides are not low iron glass as used previously [9], but were chosen for ease of handling with the integrating sphere sample mount.

A. Optical Uniformity

The area coverage of each coupon was evaluated using an optical microscope and image processing software. A set of three images at 2.52x magnification was collected at the center of each coupon. Typical micrographs are shown in Fig. 1, corresponding to light (Fig. 1a) and heavy (Fig. 1b) coatings. The coupons are shown in Fig. 1c. The correlation between applied sand loading and the obscured area was measured using image analysis of each coupon. A logarithmic trend was observed for each series, as shown in Fig. 2. As the mass of applied sand increases, a proportional percentage of the unit area is covered, preventing light transmission. Soil coverage eventually reaches an asymptote, 100% area coverage. Hegazy [10] used an error function with empirical coefficients to describe the transmission loss due to soil accumulated over a one-month period. However; soil contains a range of particle sizes, shapes, and compositions, each of which can influence the rate of aggregate formation.

A general form of the equation used is shown in eq. (4).

$$Coverage = 100 - \text{erf}(bx^c) \tag{4}$$

The magnitude is fixed at 100% coverage, and coefficients b and c are used to adjust the curve accordingly. A trend relating the coefficients to extent of patterning could not be determined from the available data (Fig. 2). At very minimal soil coverage, the texture is dominated by individual particulates (Fig. 1a). At heavy soil coatings, macroscopic patterns are present (Fig. 1b), but the quantity of soil ensures that the incident beam will scatter multiple times, negating the effect of the soil texture.

B. Spray-coated Samples

Angle of incidence measurements were collected at 10° increments relative to a clean coupon at the 0° position. The measured reflectance generally decreased proportionally to the amount of sand on the coupon, as shown in Fig. 3. Since the sand contains few optically absorbing components, the incident light is scattered throughout the integrating sphere. As a result, increasing the amount of sand on the surface increases diffuse scattering. Since the sample is mounted in the center of the sphere, diffuse light will eventually be collected by the detector. Relative to the 0° position, the reflectance of a clean coupon increases until 30°, then decreases (Fig. 3). Soiled coupons exhibit a similar response where the reflectance peaks near 30°. The amount of soil was much more significant than the AOI, as seen by the gradations of area fraction in Fig. 3. Interestingly, the 60:40 sample yielded the most uniform trend.

C. Spot Soiling

In order to address uniformity and AOI effects in a more consistent manner, small soil droplets were deposited on glass slides at varying deposition densities. Solvent ratios were varied (section II-B) to control the density and patterning of the dried droplet. The applied mass was below the detection limit, so soil loadings are reported in terms of the total area of the dried soil film. Each sample prepared using ACN exhibited some degree of pattern formation (Figs. 4a to 4e), while the 0% ACN samples were homogeneous, as well as less dense (Fig. 4f) due to a greater total area coverage. The lower volatility solvent spread over a larger area before

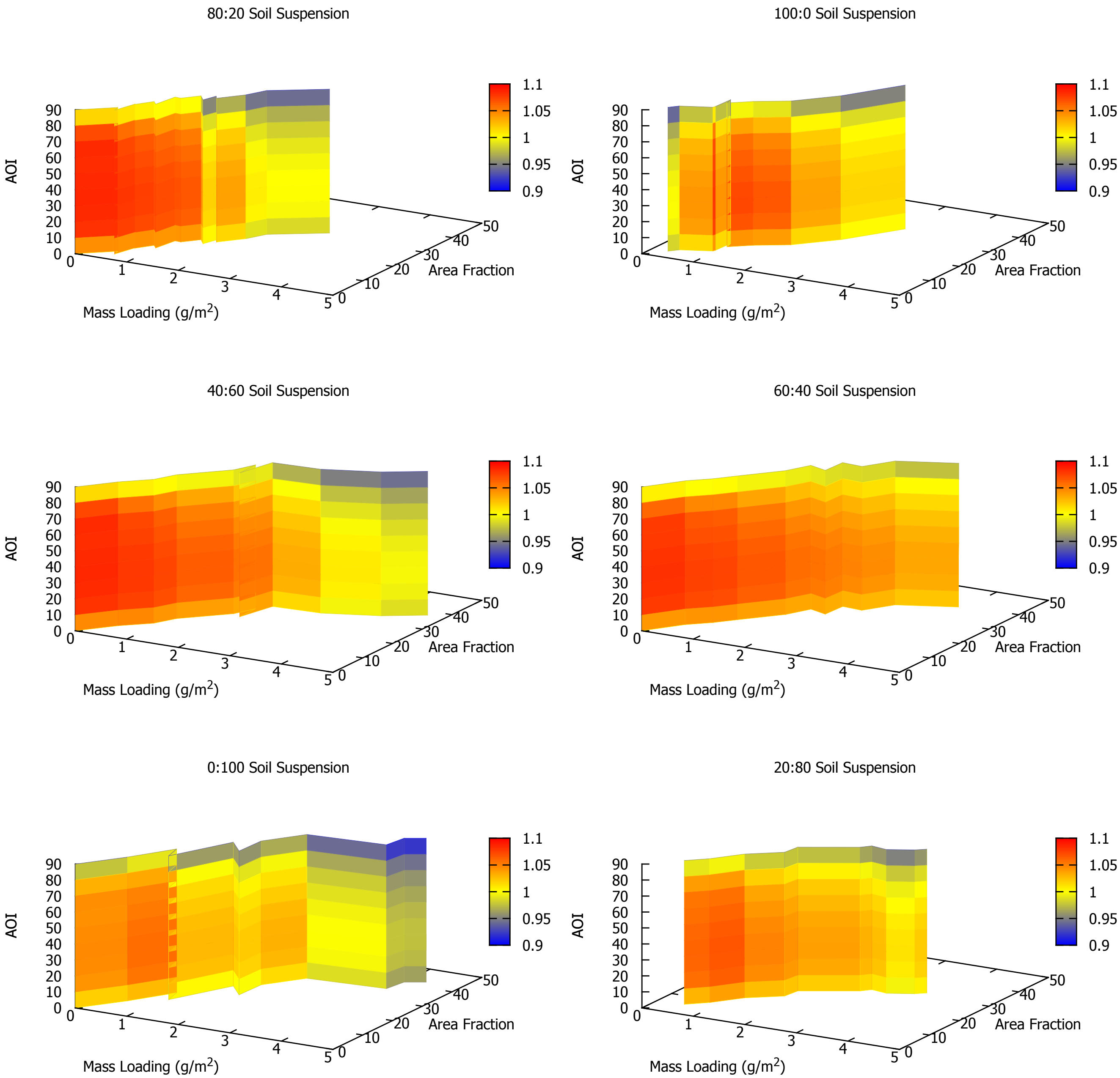

Fig. 3. Integrated reflectance of soiled coupons at 0-90° AOI for each solvent-patterned soil series. Solvent type (EtOH:ACN) is indicated in each title. Measured intensity, relative to a clean coupon at 0° is indicated by the color bar. Generally, intensity decreases as AOI and area coverage increase.

it evaporated, allowing the suspended particulates to settle slowly. In contrast, the high volatility ACN evaporated quickly, producing patterns due to particle accumulation at the drying edge. As would be expected, the 100% ACN samples exhibited this effect to the greatest extent (Fig. 4a). The magnitude of the measured transmittance was similar for the entire range of samples. The trend of each AOI response likewise remained consistent throughout the sample set, except for a change in specular reflectance. Due to the instrument geometry, specular reflectance at 0° was lost to the environment, but was collected at all other sample positions. As a result, a discontinuity is present between 0 and 10° (see Fig. 5) The specular reflectance loss (and by extension, the reduction in transmission) was comparable for all samples except those prepared using 0% ACN (100% EtOH) as the dispersion solvent, as shown in Fig. 6. The low angle (10-50°) responses for all but the 0% ACN samples were likewise similar. The overall trend held until 80°, at which point the transmittance was nearly identical

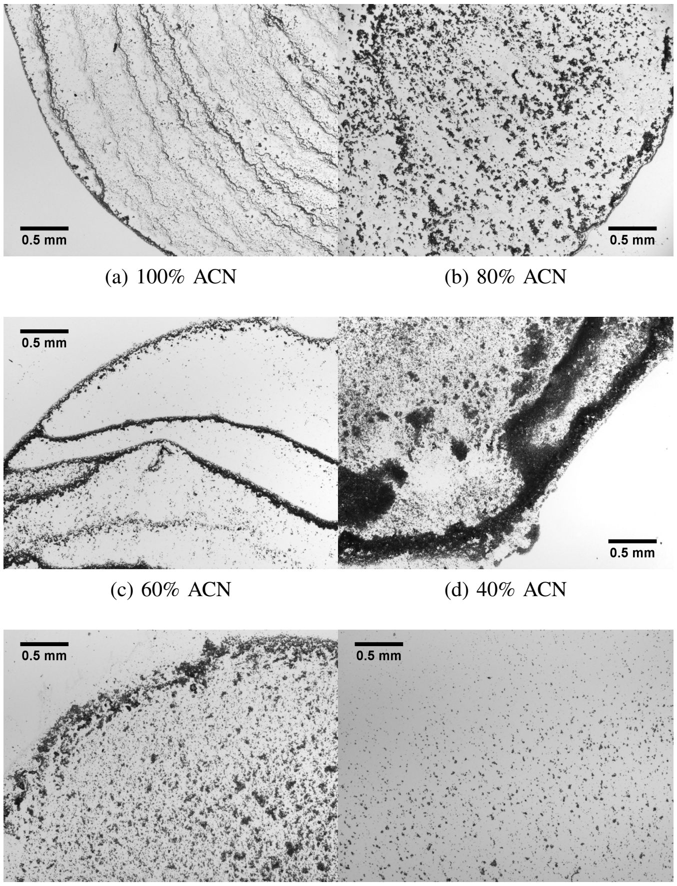

(a) 100% ACN (b) 80% ACN

(c) 60% ACN (d) 40% ACN

(e) 20% ACN (f) 0% ACN

Fig. 4. Edges of spot soiled coupons imaged at 2.52x.

for all samples. In this geometry, the edge of the soil spot is exposed to the beam, shading the remaining area. Patterning is relatively insignificant in this scenario, as very little of the soiled face is exposed to the beam. The opposite is true for the spray-coated coupons; as the majority of the glass surface is covered with soil. Once a sufficient soil loading is achieved, any region struck by the incident beam has the potential to scatter or absorb light.

The transmittance of the spot-soiled coupons can be used to illustrate an intuitive, but significant issue in soil accumulation. For a given amount of soil, losses are minimized when the particulates (or aggregates) are as dispersed as possible. No single trend could be determined among the patterned samples, except that they all exhibited a greater decrease in transmission than the 0% ACN samples with a uniform particle coverage. Particles distributed over a greater area are less prone to secondary scattering, improving overall light collection.

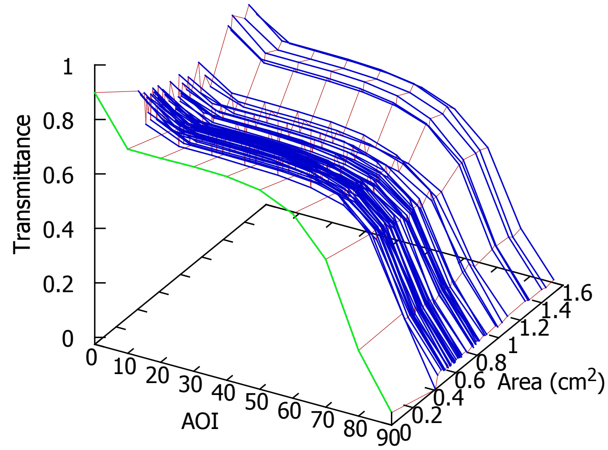

Fig. 5. Surface plot of transmittance with respect to AOI and area coverage for spot-soiled samples. The clean reference is shown in green at 0 cm^2.

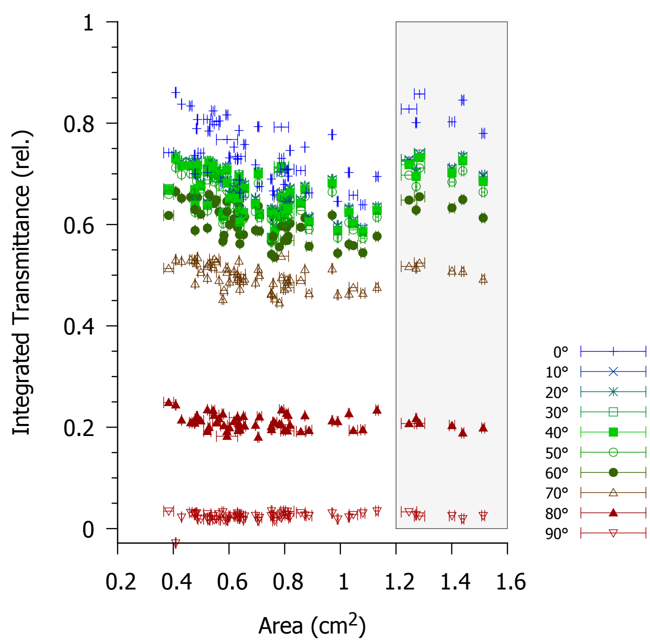

Fig. 6. AOI response of spot-soiled coupons. The 0% ACN data points are within the shaded region.

IV. Conclusion

The amount of accumulated soil and the dispersion over the surface are critical aspects to PV soiling losses. A decrease in transmission was observed for the spray-coated samples as soiling and AOI were increased, respectively. Due to the density of the deposited soil, specific trends in patterning could not be determined. Smaller scale experiments were conducted using single droplets of soil suspended in mixed solvents. The only discernible trend in patterning was an increase in transmittance for the most dispersed soils.

Acknowledgment

SAND2015-XXXX This work was supported by the U.S. Department of Energy SunShot Initiative. Sandia National Laboratories is a multi-program laboratory managed and operated by Sandia Corporation, a wholly owned subsidiary of Lockheed Martin Corporation, for the U.S. Department of Energy's National Nuclear Security Administration under contract DE-AC04-94AL85000.

References

[1] L. L. Kazmerski, M. Al Jardan, Y. Al Jnoobi, Y. Al Shaya, and J. J. John, "Ashes to ashes, dust to dust: Averting a potential showstopper for solar photovoltaics," in *Photovoltaic Specialist Conference (PVSC), 2014 IEEE 40th*, 2014, pp. 0187–0192.

[2] A. Kimber, L. Mitchell, S. Nogradi, and H. Wenger, "The Effect of Soiling on Large Grid-Connected Photovoltaic Systems in California and the Southwest Region of the United States," in *Photovoltaic Energy Conversion, Conference Record of the 2006 IEEE 4th World Conference on*, vol. 2, 2006, pp. 2391–2395.

[3] T. Sarver, A. Al-Qaraghuli, and L. L. Kazmerski, "A comprehensive review of the impact of dust on the use of solar energy: History, investigations, results, literature, and mitigation approaches," *Renewable and Sustainable Energy Reviews*, vol. 22, no. 0, pp. 698–733, 2013.

[4] E. Lorenzo, R. Moretón, and I. Luque, "Dust effects on PV array performance: in-field observations with non-uniform patterns," *Progress in Photovoltaics: Research and Applications*, pp. n/a–n/a, 2013, hot spots due to uneven shading.

[5] E. E. van Dyk, E. L. Meyer, F. J. Vorster, and A. W. R. Leitch, "Long-term monitoring of photovoltaic devices," *Renewable Energy*, vol. 25, no. 2, pp. 183–197, 2002.

[6] M. Drif, P. J. Prez, J. Aguilera, and J. D. Aguilar, "A new estimation method of irradiance on a partially shaded pv generator in grid-connected photovoltaic systems," *Renewable Energy*, vol. 33, no. 9, pp. 2048–2056, 2008.

[7] W. S. Rasband, "ImageJ," 1997-2012. [Online]. Available: http://imagej.nih.gov/ij/

[8] S. L. Storm, A. Springsteen, and T. M. Ricker, "The use of center mount sample holders in reflectance spectroscopy," 1998.

[9] P. D. Burton and B. H. King, "Spectral Sensitivity of Simulated Photovoltaic Module Soiling for a Variety of Synthesized Soil Types," *Photovoltaics, IEEE Journal of*, vol. 4, no. 3, pp. 890–898, 2014.

[10] A. A. Hegazy, "Effect of dust accumulation on solar transmittance through glass covers of plate-type collectors," *Renewable Energy*, vol. 22, no. 4, pp. 525–540, 2001.